

Dynamics of the Rocking Frame with Vertical Restrainers

Nicos Makris, M.ASCE¹; and Michalis F. Vassiliou²

Abstract: This paper investigates the rocking response and stability analysis of an array of slender columns capped with a rigid beam which are vertically restrained with elastic prestressed tendons that pass through the centerline of the columns while anchored at the foundation and the cap-beam. Following a variational formulation, the nonlinear equation of motion is derived in which the stiffness and the prestressing force of the tendons are treated separately. In this way, the postuplift stiffness of the vertically restrained rocking frame can be anywhere from negative to positive depending on the axial stiffness of the vertical tendons. The paper shows that the tendons are effective in suppressing the response of rocking frames with small columns subjected to long-period excitations. As the size of the columns, the frequency of the excitations, or the weight of the cap-beam increases, the vertical tendons become immaterial given that most of the seismic resistance of tall rocking frames originates primarily from the mobilization of the rotational inertia of their columns. The paper concludes with the presentation and validation of an equivalent rigid-linear system so that the rocking response of vertically restrained rocking frames can be computed with popular open-source or commercially available software simply by employing existing elastic-multilinear elements. DOI: 10.1061/(ASCE)ST.1943-541X.0001231. © 2014 American Society of Civil Engineers.

Introduction

The design of most modern structural framing systems is based on three basic concepts that are deeply rooted in structural engineering. The first concept is that of creating statically indeterminate (redundant) framing systems. When a “statically indeterminate” structure is subjected to strong lateral loads and some joints develop plastic hinges, there is enough redundancy in the system that other joints maintain their integrity. The second concept, known as ductility, is the ability of the structure to maintain sufficient strength at large deformations. In this way, in the event of excessive lateral loads that may convert all joints into plastic hinges, the ductile behavior prevents collapse; however, in this case the structure may experience appreciable permanent displacements together with severe damage at the hinge zones. Therefore, in a strong earthquake irreparable damage to structures is inevitable with this design philosophy. The third concept that dominates modern structural engineering is that of positive stiffness. When a structure behaves elastically, forces and deformations are proportional. When yielding is reached, the forces are no longer proportional to the deformations; however, in most cases the stiffness at any instant of the deformation history of the structure remains positive—that is, if some force is needed to keep the structure away from equilibrium at some displacement, then a larger force is needed to keep the structure away from equilibrium at a larger displacement.

Fig. 1(a) illustrates the deformation pattern of a moment-resisting, fixed base frame when subjected to a lateral load capable

of inducing yielding at the joints. The force-deformation curve ($P-u$) is nonlinear and the behavior is ductile; nevertheless, the lateral stiffness of the system remains positive at all times.

Along with the moment-resisting, ductile frame, Fig. 1(b) illustrates the deformation pattern of a freestanding, rocking frame (two freestanding rigid columns capped with a freely supported rigid beam) when subjected to a lateral load capable of inducing uplifting of the columns. The force-displacement relationship ($P-u$) of the rotating frame shown at the bottom of Fig. 1(b) indicates that the articulated system has “infinite” stiffness until uplift is induced and, once the four-hinge frame is set into rocking motion, its restoring force decreases monotonically, reaching zero when the rotation of the columns, $\theta = \alpha = \arctan(b/h)$. Accordingly, the freestanding rocking frame shown in Fig. 1(b) is a four-hinge mechanism that exhibits negative lateral stiffness. Furthermore, during the oscillatory rocking motion of a freestanding rocking frame, the force-displacement curve does not enclose any area; therefore, the ductility of the system is zero given that energy is lost only during impact when the angle of rotation reverses.

In summary, Fig. 1 indicates that, whereas most modern structural engineers are trained to design statically indeterminate and ductile structures that exhibit positive stiffness, ancient builders were designing entirely different structural systems—that is, articulated mechanisms that exhibit marginal ductility and negative stiffness. What is remarkable about these “unconventional” articulated structures, such as the Late Archaic Temple of Aphaia in the island of Aegina near Athens (Makris and Vassiliou 2013), is that they have endured the test of time by surviving several strong seismic motions during their 2.5-millenia life. Recently the concept of negative stiffness has received increasing attention for the seismic protection of structures, to the extent that elaborate mechanical assemblies [negative stiffness device (NSD)] that involve highly compressed springs have been proposed (Pasala et al. 2012; Sarlis et al. 2012).

Despite the documented remarkable seismic performance of ancient articulated temples (Konstantinidis and Makris 2005; Papaloizou and Komodromos 2009; Ambraseys and Psycharis 2011; Vassiliou and Makris 2012; Makris and Vassiliou 2013, 2014; DeJong and Dimitrakopoulos 2014), the number of modern structures that have been intentionally designed to rock on their

¹Professor, Dept. of Civil, Environmental and Construction Engineering, Univ. of Central Florida, P.O. Box 162450, Orlando, FL 32816-2450; and Dept. of Civil Engineering, Univ. of Patras, GR-26500, Greece (corresponding author). E-mail: nmakris@upatras.gr

²Postdoctoral Researcher, Institute of Structural Engineering IBK, Wolfgang-Pauli-Strasse 15, Swiss Federal Institute of Technology ETH Zürich, CH-8093 Zürich, Switzerland; formerly, Ph.D. Student, Dept. of Civil Engineering, Univ. of Patras, GR-26500, Greece.

Note. This manuscript was submitted on February 23, 2014; approved on November 18, 2014; published online on December 24, 2014. Discussion period open until May 24, 2015; separate discussions must be submitted for individual papers. This paper is part of the *Journal of Structural Engineering*, © ASCE, ISSN 0733-9445/04014245(13)/\$25.00.

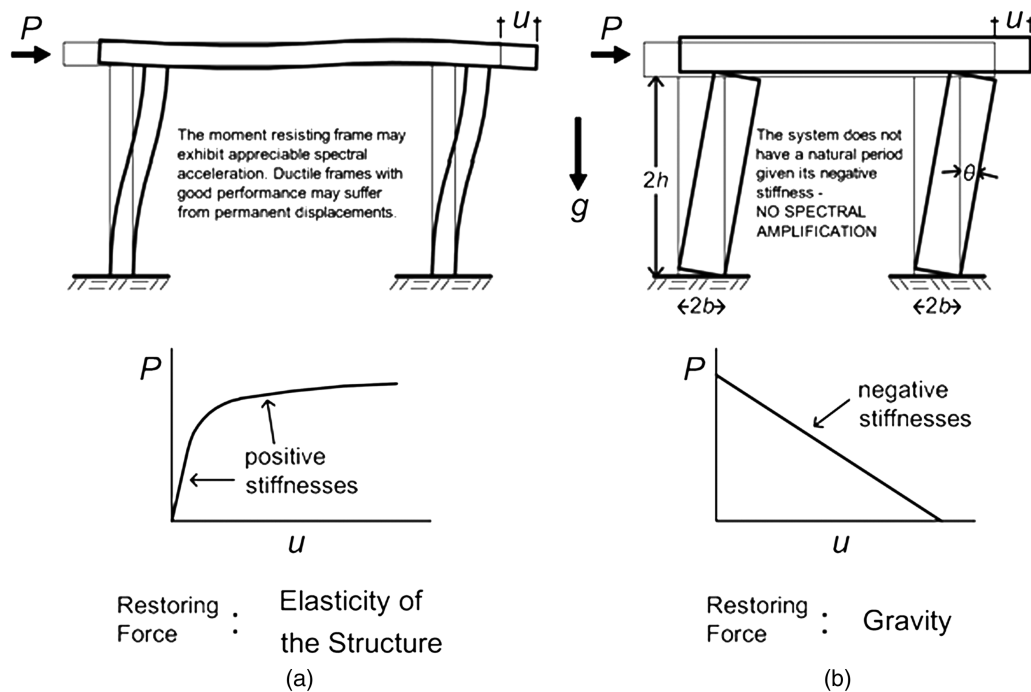


Fig. 1. Fundamental difference in the behavior of (a) a traditional moment-resisting frame; (b) a rocking frame with freestanding columns that are allowed to rock

foundations is limited (Mander and Cheng 1997; Chen et al. 2006; Cheng 2008). Two state-of-the-practice examples may be found in New Zealand: the South Rangitikei Railway Bridge (Beck and Skinner 1973), and an industrial chimney at the Christchurch Airport (Sharpe and Skinner 1983). Along the same concept is the design of the piers of the Rion–Antirion Bridge in Greece (Pecker 2005).

In view of the appreciable damage to the hinge zones and the resulting permanent lateral displacements that are inherent to current seismic-resistant, ductile design practice, during the last two decades there has been a growing effort to rediscover the unique advantages of rocking structures. Mander and Cheng (1997) introduced the damage avoidance design (DAD), where the columns of a frame are allowed to rock on both the pile cap and the pier cap without inducing damage. This is achieved by terminating the longitudinal reinforcement of the columns before reaching the beam-column and the column-foundation interfaces. In the DAD, central post-tensioned steel tendons inside the columns are provided to increase lateral resistance, as shown in Figs. 2(a and b). In fact, the force-deformation curve presented in Fig. 2.2 of Mander and Cheng (1997) indicates that the axial stiffness of the steel tendon is large enough that the postuplift stiffness of the rocking frame is positive. By introducing such a stiff tendon that reverses the negative stiffness associated with rocking, one creates a stronger system; nevertheless, at present it is not well understood to what extent stiff vertical tendons that offer a positive lateral stiffness enhance the seismic stability of the rocking frame. A subsequent publication by Cheng (2008) presented shaking-table test results from the seismic response of a two-column rocking frame with vertical restrainers. The effect of the various parameters of the system was examined in detail, and although some configurations in the Cheng (2008) study maintained negative stiffness (i.e., the R30PNK250 test), the physical significance and the effect of increasing the stiffness of the tendon were not discussed.

The pressing need for bridges to recenter after a strong seismic event motivated several studies (Palermo et al. 2005;

Mahin et al. 2006; Sakai et al. 2006; Cheng 2007; Kam et al. 2010 and references therein), which invariably used the basic concept of restraining the bridge piers with vertical tendons and reducing or even terminating the longitudinal reinforcement of the columns before reaching their bottom and top interfaces, as was originally proposed by Mander and Cheng (1997). The same idea became popular in prefabricated-bridge technology, where again the bridge piers of the so-called hybrid rocking frame are connected to the foundation and the deck with vertically post-tensioned tendons that pass through the axis of the column together with a lighter longitudinal mild-steel reinforcement that runs near the circumference of the columns (Wacker et al. 2005; Cohagen et al. 2008, among others). With this design, during earthquake loading most of the deformation is concentrated at the pier–foundation and pier–cap–beam interfaces and the overall deformation pattern of the post-tensioned frame resembles the deformation pattern of the freestanding rocking frame (Makris and Vassiliou 2013, 2014). Nevertheless, the prevailing practice is to offer the hybrid rocking frame enough lateral moment resistance so that its lateral stiffness is invariably positive.

More than a decade ago, Makris and Zhang (2001) and Makris and Black (2002) investigated the rocking response and overturning of anchored rigid blocks and equipment, and concluded that vertical restrainers are more effective in preventing the overturning of small blocks when subjected to low-frequency pulses. As the size of the block increases, its rotational inertia increases with the square of its size, and the seismic stability of large, freestanding columns originates primarily from the difficulty in mobilizing their large rotational inertia rather than from marginal contribution of the restrainers. Part of the motivation of this study is to build on Makris and Zhang's (2001) and Makris and Black's (2002) work and bring forward that the ample seismic resistance of tall rocking frames with heavy cap-beams atop originates primarily from the difficulty in mobilizing the large rotational inertia of the system (Makris 2014) when the effect of vertical restraining tendons becomes more marginal as the size of the columns of the rocking frame increases.

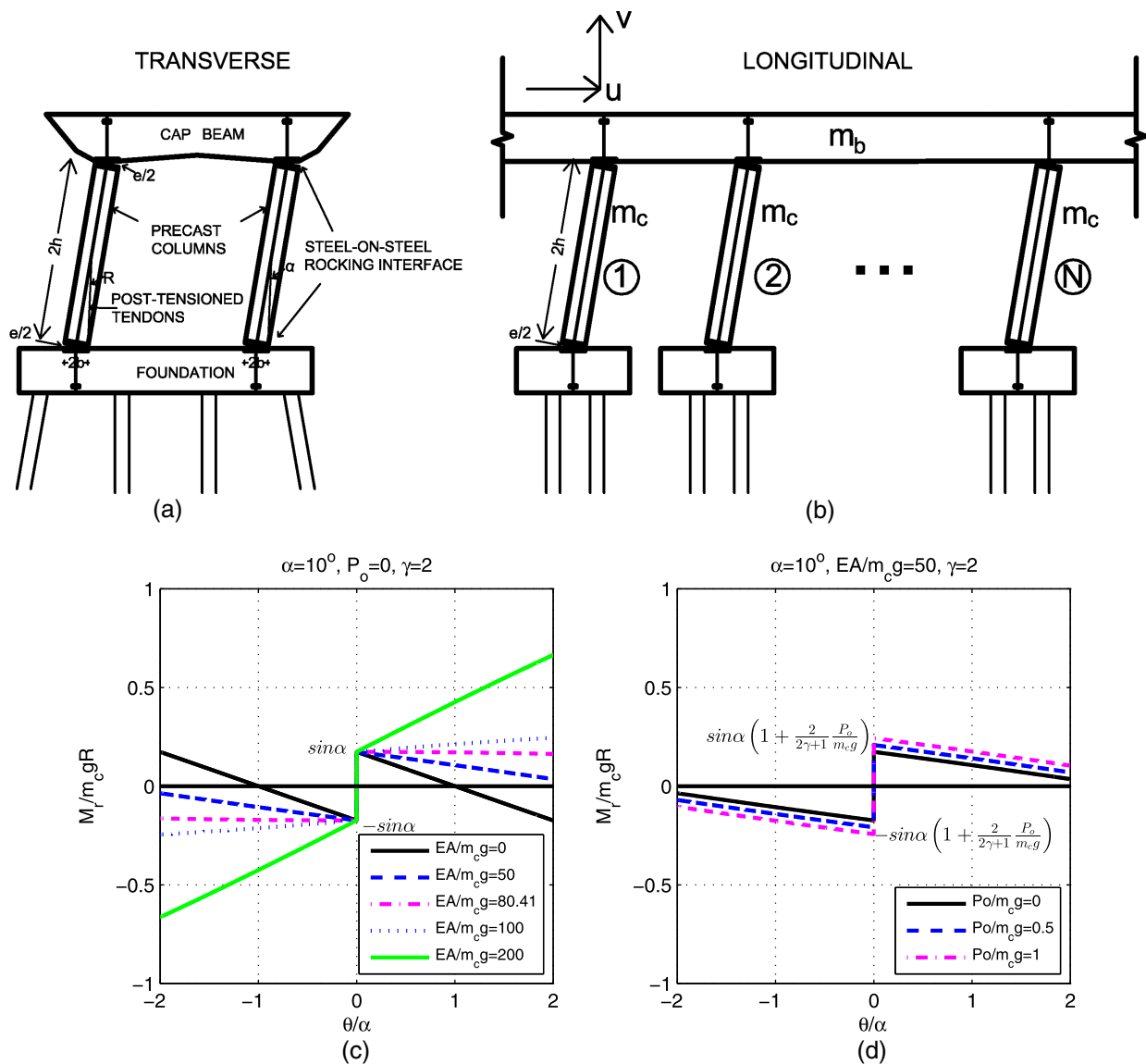


Fig. 2. (a) Transverse and (b) longitudinal sections of the vertically restrained rocking frame together with moment-rotation diagrams for various values of the dimensionless stiffness of (c) tendon $EA/m_c g$; (d) dimensionless prestressing force $P_o/m_c g$

Dynamics of the Vertically Restrained Rocking Frame

The main motivation for this study is to establish the dynamics of the vertically restrained rocking frame, which emerges as a most promising alternative design concept for tall bridges (Mander and Cheng 1997; Cheng 2008). This analysis goes beyond the one-bay configuration introduced in Mander and Cheng (1997), which essentially represents the transverse motion of the bridge system as shown in Fig. 2(a) and examines the planar rocking response of an array of N identical vertically restrained columns capped with a rigid beam that is clamped with vertical restrainers. This configuration, shown in Fig. 2(b), idealizes the longitudinal motion of a multispan bridge.

When the elasticity, EA , of the restrainer is small compared to the weight of the rocking columns, $m_c g$, on uplifting, the lateral stiffness of the system remains negative as in the free rocking case. As EA increases, the lateral stiffness of the rocking frame increases gradually from negative to positive as shown in Fig. 2(c).

Assuming that the rocking column will not topple, it will recenter, impact will happen at the new pivot point, and subsequently the column will rock with opposite rotations. During rocking, the dependent variables $u(t)$ and $v(t)$ of the center of mass of the cap-beam with mass m_b are given for $\theta(t) < 0$ and $\theta(t) > 0$ by the following expressions:

$$u(t) = \mp 2R[\sin \alpha - \sin(\alpha \pm \theta)] \quad (1)$$

$$v(t) = 2R[\cos(\alpha \pm \theta) - \cos \alpha] \quad (2)$$

In these equations, whenever there is a double sign (say \pm) the top sign is for $\theta < 0$ and the bottom sign is for $\theta > 0$. Regardless of the sign of the rotation $\theta(t)$, during an admissible rotation $\delta\theta$ the variation of the work δW done by the external filed forces is

$$\delta W = \left(m_b + \frac{N}{2} m_c\right) (\ddot{u}_g \delta u + g \delta v) \quad (3)$$

Case 1: $\theta(t) < 0$

During an admissible rotation $\delta\theta$, the variation of the work, δW , and the variations of the displacements, δu and δv , are

$$\delta W = \frac{dW}{d\theta} \delta\theta \quad (4)$$

$$\delta u = \frac{du}{d\theta} \delta\theta \quad (5)$$

$$\delta v = \frac{dv}{d\theta} \delta\theta \quad (6)$$

After differentiating Eqs. (1) and (2) for $\theta < 0$ with respect to the independent variable, θ , Eqs. (5) and (6) give

$$\delta u = 2R \cos(\alpha + \theta) \delta\theta \quad (7)$$

$$\delta v = -2R \sin(\alpha + \theta) \delta\theta \quad (8)$$

Substitution of Eqs. (7) and (8) into Eq. (3) in association with Eq. (4) gives

$$\frac{dW}{d\theta} = 2R \left(m_b + \frac{N}{2} m_c \right) [\ddot{u}_g \cos(\alpha + \theta) - g \sin(\alpha + \theta)], \quad \theta < 0 \quad (9)$$

During the rocking motion of the vertically restrained rocking frame, in addition to the work of the external field forces, W , there is work done by the axial force in the tendon, $P = (EA/2h)e$, where e is the elongation of the tendon due to the rocking motion. With reference to Figs. 2(a and b),

$$e = 2R \sin \alpha \sqrt{2(1 - \cos \theta)} \quad (10)$$

In this configuration, where the tendons also clamp the horizontal beam, the elongation in the tendons is twice the elongation during the uplift of the restrained solitary column (Vassiliou 2010).

In addition to the elongation, e , included in this analysis is an initial elongation, e_o , in the tendon due to an initial prestressing, $P_o = (EA/2h)e_o$. Accordingly, regardless of the sign of the rotation $\theta(t)$, the potential energy due to the axial force along the tendon is

$$V = \frac{1}{2} \frac{EA}{2R \cos \alpha} (e + e_o)^2 \quad (11)$$

Substitution of Eq. (10) into Eq. (11) and differentiation with respect to the independent variable, θ , yields

$$\frac{dV}{d\theta} = 2R \sin \alpha \sin \theta \left(EA \tan \alpha + \frac{P_o}{\sqrt{2 - 2 \cos \theta}} \right) \quad (12)$$

During rocking motion, Lagrange's equation should be satisfied

$$\frac{d}{dt} \left(\frac{dT}{d\dot{\theta}} \right) - \frac{dT}{d\theta} = - \frac{dW}{d\theta} - \frac{dV}{d\theta} \quad (13)$$

In this equation, T is the kinetic energy of the system whereas $dW/d\theta$ and $dV/d\theta$ are given by Eqs. (9) and (12), respectively. In either case, $\theta(t) < 0$ or $\theta(t) > 0$, the kinetic energy of the system is

$$T = \frac{N}{2} I_o \dot{\theta}^2(t) + \frac{1}{2} m_b [\dot{u}(t)^2 + \dot{v}(t)^2] \quad (14)$$

The substitution of Eqs. (9), (12), and (14) into Lagrange Eq. (13) results in the equation of motion of the vertically restrained rocking frame for $\theta(t) < 0$

$$\begin{aligned} \frac{2}{3} R(1 + 3\gamma) \ddot{\theta}(t) = & - \left(\frac{1}{2} + \gamma \right) [\ddot{u}_g \cos(\alpha + \theta) - g \sin(\alpha + \theta)] \\ & - \sin \alpha \sin \theta \left(\frac{EA}{m_c} \tan \alpha + \frac{P_o}{m_c \sqrt{2 - 2 \cos \theta}} \right) \end{aligned} \quad (15)$$

where $\gamma = m_b/Nm_c$.

Eq. (15) simplifies to

$$\begin{aligned} \ddot{\theta}(t) = & - \frac{1 + 2\gamma}{1 + 3\gamma} p^2 \left[- \sin(\alpha + \theta) + \frac{\ddot{u}_g}{g} \cos(\alpha + \theta) \right] \\ & - \frac{2}{1 + 3\gamma} p^2 \sin \alpha \sin \theta \left(\frac{EA}{m_c g} \tan \alpha + \frac{P_o}{m_c g \sqrt{2 - 2 \cos \theta}} \right) \end{aligned} \quad (16)$$

where $p = \sqrt{m_c R g / I_o}$ = frequency parameter of the solitary columns. For a rectangular column, $I_o = 4/3 m_c R^2$ and the frequency parameter assumes the value $p = \sqrt{3g/4R}$.

Case 2: $\theta(t) > 0$

For the case where the rotation is positive [$\theta(t) > 0$], the variation of the work, δW , done by the external field forces on the rocking frame is given again by Eq. (3) whereas, according to Eqs. (1) and (2), the variations of the dependent variables u and v are

$$\delta u = 2R \cos(\alpha - \theta) \delta\theta \quad (17)$$

$$\delta v = 2R \sin(\alpha - \theta) \delta\theta \quad (18)$$

By following a similar derivation as for the case $\theta(t) < 0$, the equation of motion of the vertically restrained rocking frame for $\theta(t) > 0$ is

$$\begin{aligned} \ddot{\theta}(t) = & - \frac{1 + 2\gamma}{1 + 3\gamma} p^2 \left[\sin(\alpha - \theta) + \frac{\ddot{u}_g}{g} \cos(\alpha - \theta) \right] \\ & - \frac{2}{1 + 3\gamma} p^2 \sin \alpha \sin \theta \left(\frac{EA}{m_c g} \tan \alpha + \frac{P_o}{m_c g \sqrt{2 - 2 \cos \theta}} \right) \end{aligned} \quad (19)$$

Eq. (16), for $\theta(t) < 0$, and Eq. (19), for $\theta(t) > 0$, can be expressed in a compact equation:

$$\begin{aligned} \ddot{\theta}(t) = & - \frac{1 + 2\gamma}{1 + 3\gamma} p^2 \left[\sin(\alpha \text{sgn} \theta - \theta) + \frac{\ddot{u}_g}{g} \cos(\alpha \text{sgn} \theta - \theta) \right] \\ & - \frac{2}{1 + 3\gamma} p^2 \sin \alpha \sin \theta \left(\underbrace{\frac{EA}{m_c g} \tan \alpha}_{\text{elasticity}} + \underbrace{\frac{P_o}{m_c g \sqrt{2 - 2 \cos \theta}}}_{\text{prestressing}} \right) \end{aligned} \quad (20)$$

The first bracket in Eq. (20) describes the dynamics of the free standing rocking frame (Makris and Vassiliou 2013, 2014); the second bracket describes the contribution of the vertical tendons.

During the oscillatory rocking motion of the vertically restrained rocking frame, the moment-rotation behavior that depends on the elasticity of the tendons and the level of prestressing is expressed with one of the curves shown in Figs. 2(c and d) that do not enclose any area. Energy is lost only during impact, when the angle of rotation reverses. It is assumed that, at this instant, the rotation continues smoothly and that the impact forces concentrate at the new pivot points at the base and heads of the columns. During

impact [$\theta(t) = 0$] the elongation of the tendon, e , given by Eq. (10) is zero, and any finite force due to prestressing assumes the same value before and after the impact. Accordingly, any forces in the tendons at the instant of impact do not create any change in the moment of momentum before and after the impact. Following this reasoning, the ratio of the kinetic energy of the rocking frame before and after the impact is offered by the same expression that was derived in Makris and Vassiliou (2013) from the conservation of the moment of momentum of the freestanding rocking frame (no vertical restrainers):

$$r = \frac{\dot{\theta}_2^2}{\dot{\theta}_1^2} = \left(\frac{1 - \frac{3}{2} \sin^2 \alpha + 3\gamma \cos 2\alpha}{1 + 3\gamma} \right)^2 \quad (21)$$

Effect of the Restraining Tendons and the Mass of the Cap-Beam

The mathematical structure of Eq. (20) offers some valuable information regarding the effectiveness of vertical restrainers in association with column size and cap-beam weight. The term associated with the first bracket of Eq. (20) expresses the dynamics of the freestanding rocking frame (Makris and Vassiliou 2013, 2014). The quantity $\hat{p} = \sqrt{(1 + 2\gamma/1 + 3\gamma)}p$ is the frequency parameter of the freestanding rocking frame showing that its dynamic response is identical to the rocking response of a single freestanding column with the same slenderness but with a larger size—that is, a more stable configuration.

The term associated with the second bracket of Eq. (20) expresses the contribution of the vertical restrainers. As the size of the columns increases (smaller p), the effectiveness of the vertical restrainers is suppressed with p^2 ; the effectiveness of the restrainers further reduces as the weight of the cap-beam increases (large γ). Simply stated, the combination of a heavy deck atop tall columns enhances the seismic stability of the freestanding rocking frame and reduces the effectiveness of the vertical restrainers.

On the other hand, at the limiting case of a massless rigid cap-beam ($\gamma = 0$), Eq. (20) indicates that the vertically restrained rocking frame experiences an apparent restraining stiffness that is four times larger and an apparent prestressing force that is two times larger than the corresponding values of the solitary rocking column that is vertically restrained with the same tendon [same $EA/m_c g$ and same $P_o/m_c g$; (Vassiliou 2010)].

From Negative to Positive Stiffness

In the vertically restrained rocking frame, the negative stiffness originates from the fact that as the rotation increases the restoring weight vectors of the columns and the cap-beam approach the pivot point; the positive stiffness originates from the presence of the vertical elastic restrainers, which offer an increasing restoring moment.

Without loss of generality, the focus here is the case of positive rotations [$\theta(t) > 0$]. Eq. (19) indicates that the rotation-dependent restoring moment is

$$M(\theta) = m_c g R \left[\sin(\alpha - \theta) + \frac{2}{1 + 2\gamma} \sin \alpha \sin \theta \left(\tan \alpha \frac{EA}{m_c g} + \frac{1}{\sqrt{2}\sqrt{1 - \cos \theta}} \frac{P_o}{m_c g} \right) \right] \quad (22)$$

Using $\sin(\alpha - \theta) = \sin \alpha \cos \theta - \cos \alpha \sin \theta$, after rearranging terms Eq. (22) assumes the form

$$\frac{M(\theta)}{m_c g R} = \sin \alpha \left[\cos \theta + \sin \theta \left(\frac{2}{2\gamma + 1} \tan \alpha \frac{EA}{m_c g} + \frac{2}{2\gamma + 1} \frac{1}{\sqrt{2}\sqrt{1 - \cos \theta}} \frac{P_o}{m_c g} - \cot \alpha \right) \right] \quad (23)$$

Fig. 2(c) plots the expression given by Eq. (23) for various values of the dimensionless elastic force $EA/m_c g$ for a column with slenderness $\alpha = 10^\circ$. Clearly, as the elasticity of the tendon increases, the slope of the restoring moment goes from negative to positive. Furthermore, Figs. 2(c and d) reveal that, whereas the right-hand side of Eq. (23) is nonlinear, the restoring moment exhibits a nearly linear dependence with the rotation θ . For small rotations, $1 - \cos \theta \approx \theta^2/2$, and given that Eq. (23) is for $\theta(t) > 0$, the term $\sqrt{2}\sqrt{1 - \cos \theta} \approx \theta$. Accordingly, Eq. (23) gives

$$\frac{M(\theta)}{m_c g R} = \sin \alpha \left[\cos \theta + \frac{\sin \theta}{\theta} \frac{2}{2\gamma + 1} \frac{P_o}{m_c g} + \sin \theta \left(\frac{2}{2\gamma + 1} \tan \alpha \frac{EA}{m_c g} - \cot \alpha \right) \right] \quad (24)$$

Eq. (24) is further linearized up to first-order terms by taking $\sin \theta \approx \theta$ and $\cos \theta \approx 1$

$$\frac{M(\theta)}{m_c g R} = \sin \alpha \left[1 + \frac{2}{2\gamma + 1} \frac{P_o}{m_c g} + \theta \left(\frac{2}{2\gamma + 1} \tan \alpha \frac{EA}{m_c g} - \cot \alpha \right) \right] \quad (25)$$

The factor of the rotation θ in Eq. (25) is the stiffness of the system on uplifting, and therefore the condition for the linearized system to exhibit a positive stiffness is

$$\frac{EA}{m_c g} > \left(\frac{1}{2} + \gamma \right) \frac{1}{\tan^2 \alpha} \quad (26)$$

For instance, when $\alpha = 10^\circ$, according to expression (26) a vertically restrained rocking frame exhibits a positive stiffness if $EA/m_c g > 48.25$ for $\gamma = 1$ and $EA/m_c g > 80.41$ for $\gamma = 2$. When inequality (26) becomes an equality, the vertically restrained rocking column exhibits a rigid-plastic behavior without enclosing any area. It can be confirmed that the linearization of the system as presented by Eq. (26) offers dependable results even for values of the rotation θ as large as the slenderness α . As an example, when one works with the nonlinear expression given by Eq. (23), the exact value of $EA/m_c g$ that keeps the derivative $dM_r(\theta)/d(\theta)$ positive is (Vassiliou 2010)

$$\frac{EA}{m_c g} > \left(\frac{1}{2} + \gamma \right) \left(\frac{1 + \tan^2 \alpha}{\tan^2 \alpha} \right) \quad (27)$$

The difference between inequalities Eqs. (26) and (27) is less than 3.0% for a rocking frame with columns having slenderness $\alpha = 10^\circ$.

Minimum Acceleration Needed to Initiate Uplift of the Vertically Restrained Rocking Frame

With reference to Fig. 2(b) during an admissible rotation, $\delta\theta$, the application of the principle of virtual work gives

$$\left(m_b + \frac{N}{2} m_c \right) \ddot{u}_g \delta u = \left(m_b + \frac{N}{2} m_c \right) g \delta v + N(P + P_o) \delta e \quad (28)$$

where N = number of columns; $P = (EA/2h)e$ = axial force in the tendon that develops during uplifting; P_o = possible initial prestressing force; and δe = first variation of the elongation, e , given by Eq. (10) and expressed as

$$\delta e = \frac{de}{d\theta} \delta\theta = 2R \sin \alpha \frac{\sin \theta}{\sqrt{2\sqrt{1 - \cos \theta}}} \delta\theta \quad (29)$$

Without loss of generality, it is assumed that the rocking frame undergoes a positive rotation [$\theta(t) > 0$]. Substitution of Eqs. (17), (18), and (29) into Eq. (28) gives

$$\left(m_b + \frac{N}{2}m_c\right) \ddot{u}_g \cos(\alpha - \theta) = \left(m_b + \frac{N}{2}m_c\right) g \sin(\alpha - \theta) + N(P + P_o) \sin \alpha \frac{\sin \theta}{\sqrt{2\sqrt{1 - \cos \theta}}} \quad (30)$$

At the initiation of uplift $\theta \approx 0$ and $e \approx 0$; therefore, Eq. (30), after dividing with Nm_c , simplifies to

$$\left(\gamma + \frac{1}{2}\right) \ddot{u}_g \cos \alpha = \left(\gamma + \frac{1}{2}\right) g \sin \alpha + \frac{P_o}{m_c} \sin \alpha \quad (31)$$

given that $\sqrt{2\sqrt{1 - \cos \theta}} \approx \theta$ and that $P = (EA/2h)e = 0$. According to Eq. (31), the minimum uplifting acceleration of the vertically restrained rocking frame is

$$\ddot{u}_g^{\text{up}} = g \tan \alpha \left(1 + \frac{2}{2\gamma + 1} \frac{P_o}{m_c g}\right) \quad (32)$$

Eq. (32) indicates that as the ratio of the weight of the deck to the weight of the columns increases (larger $\gamma = m_b/Nm_c$), the effect of the prestressing force, P_o , reduces and the uplift acceleration tends to that of the freestanding rocking frame—that is, $g \tan \alpha$ (Makris and Vassiliou 2013, 2014).

Rocking Spectra of the Vertically Restrained Rocking Frame: Self Similar Response

The various mathematical idealizations of coherent pulse-type ground motions as described in several publications over the last half century (e.g., Veletsos and Newmark 1960; Veletsos et al. 1965; Bertero et al. 1978; Hall et al. 1995; Makris 1997; Makris and Chang 2000; Alavi and Krawinkler 2001; Mavroidis and Papageorgiou 2003; Makris and Psychogios 2006; Baker 2007; Vassiliou and Makris 2011) are invariably characterized by a pulse period, T_p , and a pulse acceleration amplitude, a_p .

The current established methodologies for estimating the pulse characteristics of a wide class of records are of unique value because the product, $a_p T_p^2 = L_p$, is a characteristic length scale of the ground excitation and is a measure of the persistence of the most energetic pulse to generate inelastic deformation (Makris and Black 2004a, b). It is emphasized that the persistence of the pulse, $a_p T_p^2 = L_p$, is different from the strength of the pulse that is measured with the peak pulse acceleration, a_p . The reader may recall that among two pulses with different acceleration amplitude (say $a_{p1} > a_{p2}$) and different pulse durations (say $T_{p1} < T_{p2}$) the inelastic deformation does not scale with the peak pulse acceleration (most intense pulse) but with the strongest length scale (larger $a_p T_p^2 =$ most persistent pulse) (Makris and Black 2004a, b, Makris and Psychogios 2006; Karavassilis et al. 2010).

The pulse excitation shown as an inset in the subplots of Figs. 3 and 4 is a scaled expression of the second derivative of the

Gaussian distribution, $e^{-t^2/2}$, known in the seismological literature as the symmetric Ricker wavelet (Ricker 1943, 1944)

$$\psi(t) = a_p \left(1 - \frac{2\pi^2 t^2}{T_p^2}\right) e^{-1/2(2\pi^2 t^2/T_p^2)} \quad (33)$$

The wavelet given by Eq. (33) or its time derivative

$$\dot{\psi}(t) = \frac{a_p}{\beta} \left(\frac{4\pi^2 t^2}{3T_p^2} - 3\right) \frac{2\pi t}{\sqrt{3}T_p} e^{-1/2(4\pi^2 t^2/3T_p^2)} \quad (34)$$

satisfactorily approximates the coherent pulse of several pulse-like ground motions (Apostolou et al. 2007; Vassiliou and Makris 2011 and references therein). The value of $T_p = 2\pi/\omega_p$ is the period that maximizes the Fourier spectrum of the wavelet; the factor β in Eq. (34) is equal to 1.3801, so the antisymmetric Ricker wavelet has a maximum equal to a_p .

The choice of the specific functional expression to approximate the main pulse of pulse-type ground motions has limited significance in this work. What is important is that several strong ground motions contain a distinguishable acceleration pulse that is responsible for most of the inelastic deformation of structures (see references at the beginning of this section). A mathematically rigorous and easily reproducible methodology based on wavelet analysis to construct the best-matching wavelet was recently proposed by Vassiliou and Makris (2011).

The first two terms in the right-hand side of Eq. (20) express the response of the free standing rocking frame, which is fully described by five independent dimensionless variables (Makris and Vassiliou 2013), $\Pi_\theta = \theta$, $\Pi_\omega = \omega_p/p$, $\Pi_a = \tan \alpha$, $\Pi_\gamma = \gamma = m_b/Nm_c$, and $\Pi_g = a_p/g$, where a_p and $\omega_p = 2\pi/T_p$ are the acceleration amplitude and cyclic frequency of the excitation pulse, respectively. The contributions of the elasticity, E , and the prestressing force of the tendon, P_o , enter Eq. (20) in a dimensionless form, $\Pi_E = EA/m_c g$ and $\Pi_P = P_o/m_c g$.

With the seven dimensionless Π terms established, the dynamic response of the vertically restrained rocking frame can be expressed as

$$\theta(t) = \varphi \left(\frac{\omega_p}{p}, \tan \alpha, \gamma, \frac{a_p}{g}, \frac{EA}{m_c g}, \frac{P_o}{m_c g}\right) \quad (35)$$

Contingency of Resonance

Eq. (25) indicates that the linearized rotational stiffness of the vertically restrained rocking column is given by

$$K_r = m_c g R \sin \alpha \left(\frac{2}{2\gamma + 1} \tan \alpha \frac{EA}{m_c g} - \frac{1}{\tan \alpha}\right) \quad (36)$$

When $EA/m_c g$ is sufficiently large and satisfies inequality [Eq. (26)], K_r is positive, and on uplifting ($\theta \neq 0$) the rotational frequency of the vertically restrained rocking frame becomes

$$\omega_r^2 = \frac{m_c g R \sin \alpha \left(\frac{2}{2\gamma + 1} \tan \alpha \frac{EA}{m_c g} - \frac{1}{\tan \alpha}\right)}{I_o \frac{(1 + 3\gamma)}{(1 + 2\gamma)}} \quad (37)$$

Recognizing that $p^2 = m_c g R/I_o$ and that for slender columns $\sin \alpha \approx \tan \alpha$, Eq. (37) gives

$$\omega_r = \sqrt{\frac{1 + 2\gamma}{1 + 3\gamma}} p \sqrt{\frac{2}{2\gamma + 1} \tan^2 \alpha \frac{EA}{m_c g} - 1} \quad (38)$$

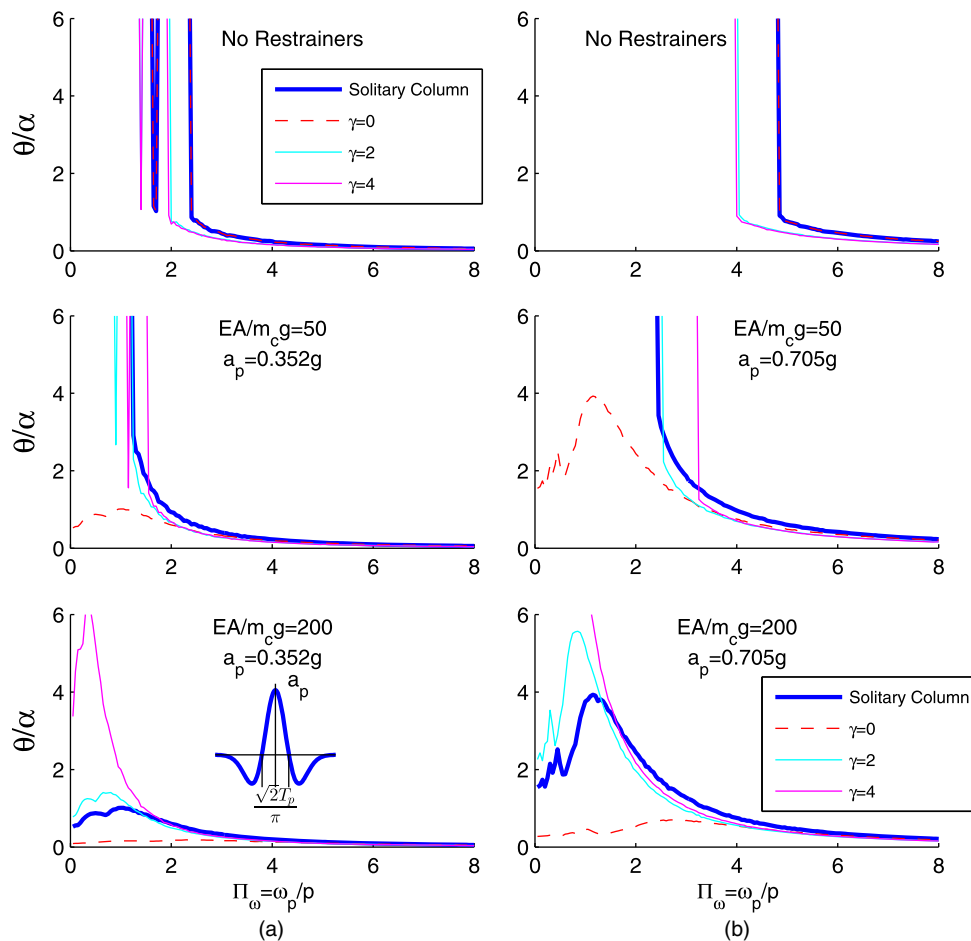


Fig. 3. Rocking spectra for different values of the dimensionless products $\Pi_g = a_p/g$, $\Pi_E = EA/m_c g$, and $\Pi_\gamma = \gamma$ when a vertically restrained rocking frame with columns having slenderness $\alpha = 10^\circ$ ($\Pi_\alpha = \tan \alpha = 0.176$) and $P_o = 0$ is subjected to a symmetric Ricker wavelet; in tall rocking frames (large values of ω_p/p) the effect of vertical restrainers is marginal: (a) $\Pi_g/\Pi_\alpha = a_p/g \tan \alpha = 2$; (b) $\Pi_g/\Pi_\alpha = a_p/g \tan \alpha = 4$

In Eq. (38), the quantity $\sqrt{1 + 2\gamma/1 + 3\gamma}p = \hat{p}$ is the frequency parameter of the freestanding rocking frame (Makris and Vassiliou 2013, 2014).

At resonance, $\omega_p = \omega_r$, and this happens when

$$\frac{\omega_p}{p} = \sqrt{\frac{1 + 2\gamma}{1 + 3\gamma}} \sqrt{\frac{2}{2\gamma + 1} \tan^2 \alpha \frac{EA}{m_c g} - 1} \quad (39)$$

or, in terms of dimensionless products, the vertically restrained rocking column is at resonance when

$$\Pi_\omega = \sqrt{\frac{1 + 2\Pi_\gamma}{1 + 3\Pi_\gamma}} \sqrt{\frac{2}{1 + 2\Pi_\gamma} \Pi_\alpha^2 \Pi_E - 1} \quad (40)$$

For instance, according to Eq. (39) when $\alpha = 10^\circ$, $\gamma = 1$, and $EA/m_c g = 100 > 48.25$, the system is at resonance when $\omega_p/p = 0.90$, whereas when $EA/m_c g = 200$ the system is at resonance when $\omega_p/p = 1.54$.

Fig. 3 shows the rocking spectra of a vertically restrained rocking frame for two levels of ground excitation ($\Pi_g/\Pi_\alpha = 2$ and 4) and three values of the elasticity of the tendon (freestanding = $EA/m_c g = 0$, 50, and 200) as the weight of the cap-beam (deck) increases ($\gamma = 0, 2$, and 4). The ground excitation is the symmetric Ricker pulse (Mexican Hat) expressed by Eq. (33). Next to the responses of the rocking frame, the response of the solitary column is

also shown. When the configuration is freestanding (no restrainers), the enhanced seismic stability of the rocking frame due to the presence of the cap-beam (deck) is shown at the top of Fig. 3. Clearly, as the weight of the cap-beam increases (larger γ), for a given value of the elasticity of the restrainers the lateral stiffness of the rocking frame decreases [Eq. (25)].

Fig. 4 shows the rocking spectra of a vertically restrained frame with slenderness $\alpha = 10^\circ$ and $\gamma = 4$ for different values of the dimensionless products Π_g , Π_E , and Π_p when subjected to a symmetric Ricker pulse (Mexican Hat wavelet). The left-hand plots are for $a_p = 0.352$ g ($\Pi_g/\Pi_\alpha = a_p/g \tan \alpha = 2$), the center plots are for $a_p = 0.528$ g ($\Pi_g/\Pi_\alpha = 3$), and the right-hand plots are for $a_p = 0.705$ g ($\Pi_g/\Pi_\alpha = 4$). All plots show that at small values of ω_p/p (rocking frames with short columns or long duration pulses), the vertically restrained frames exhibit large rotation overturning; when the stiffness is positive [$\Pi_E = EA/m_c g > \{(1/2) + \gamma\}/\tan^2 \alpha$], they exhibit the expected amplification in the neighbourhood of resonance

$$\Pi_\omega = \frac{\omega_p}{p} > \frac{\sqrt{1 + 2\gamma}}{\sqrt{1 + 3\gamma}} \sqrt{\frac{2 \tan^2 \alpha EA}{1 + 2\gamma m_c g} - 1}$$

On the other hand, as ω_p/p increases (larger columns or shorter duration pulses), the response from all configurations reduces to a

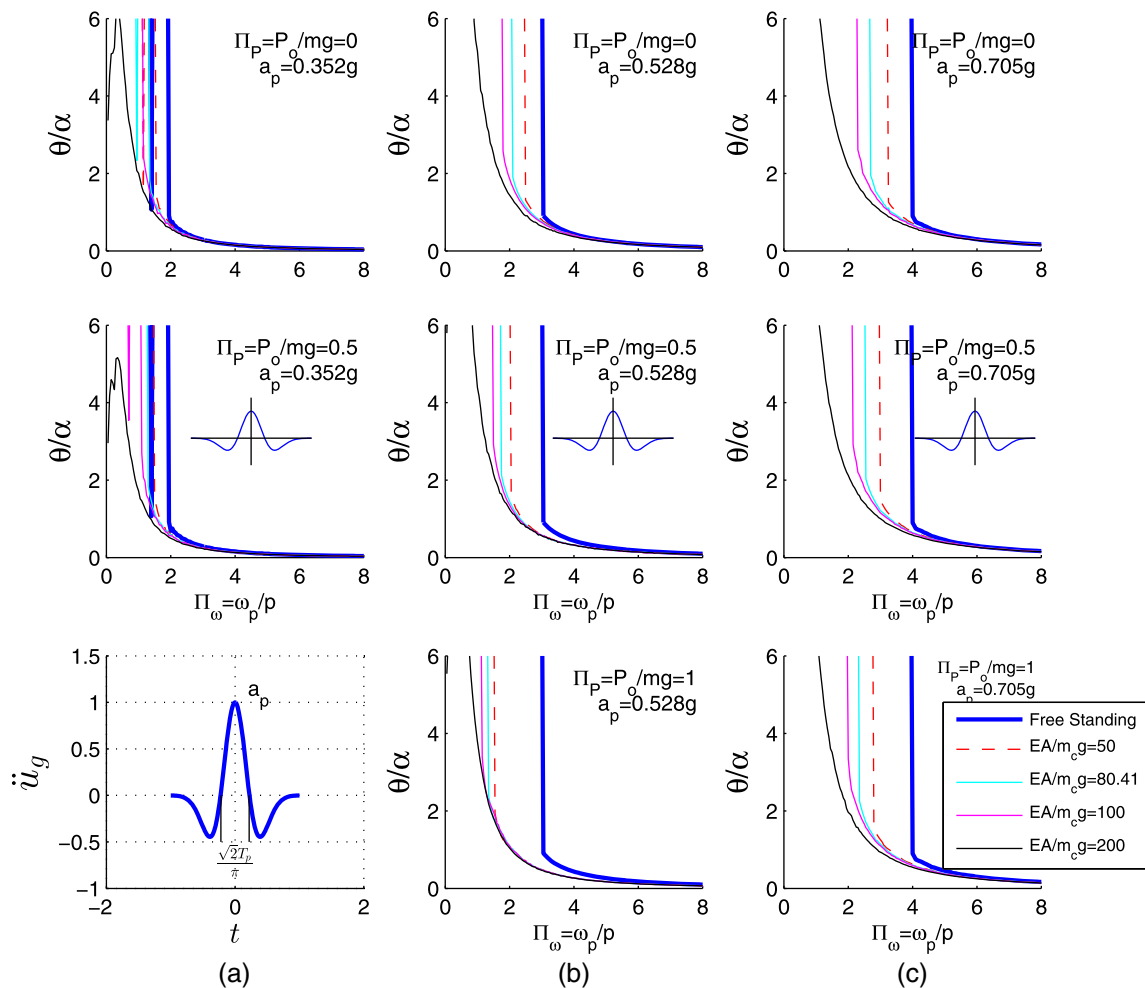


Fig. 4. Rocking spectra, $\Pi_\alpha = \tan \alpha = 0.176$ ($\alpha = 10^\circ$), $\Pi_\gamma = \gamma = 4$, for different values of the dimensionless products. $\Pi_g = a_p/g$, $\Pi_E = EA/m_c g$, and $\Pi_P = P_o/m_c g$ when the vertically restrained rocking frame with column slenderness $\alpha = 10^\circ$ ($\Pi_\alpha = \tan \alpha = 0.176$) and $\Pi_\gamma = \gamma = 4$ is subjected to a symmetric Ricker wavelet; for values of $\Pi_\omega = \omega_p/p > 4$, the response of the freestanding rocking frame is essentially identical to the response of the restrained frame, showing that for tall rocking frames the effect of vertical restrainers is marginal; (a) $\Pi_g/\Pi_\alpha = a_D/g \tan \alpha = 2$; (b) $\Pi_g/\Pi_\alpha = a_D/g \tan \alpha = 3$; (c) $\Pi_g/\Pi_\alpha = a_D/g \tan \alpha = 4$

single curve showing that the effect of the vertical restrainers becomes marginal compared to the seismic resistance that originates from the mobilization of the rotational inertia of the columns.

The same conclusion is reached from Figs. 5 and 6, which present similar trends from the dynamic response of the vertically restrained rocking frame with slenderness $\alpha = 10^\circ$ when subjected to an antisymmetric Ricker wavelet expressed by Eq. (34).

At this point it is worth translating the dimensionless products of Fig. 4 to physical quantities of typical bridges. First the case of 9.6-m-tall piers with width $2b = 1.6$ m ($R = 4.87$, $p = 1.23$ rad/s, and $\tan \alpha = 1.6/9.6 = 0.166$) is considered. These are typical dimensions for bridge piers of highway overpasses and other smaller bridges in Europe and the United States (Zhang et al. 2004; Makris and Zhang 2004). Assume that this rocking frame with $p = 1.23$ rad/s, $\tan \alpha = 0.166$, and $\gamma = 4$ is excited by the Ricker pulse that approximates the strong 1992 Erzincan, Turkey, record ($a_p = 0.35$ g, $T_p = 1.44$ s). This gives $\Pi_\omega = \omega_p/p = 2\pi/pT_p = 3.54$. Fig. 4(a), which is for $a_p = 0.352$ g, shows that at $\omega_p/p = 3.54$ the restrainer effects are marginal and that the freestanding rocking frame experiences approximately the same uplift as the vertically restrained rocking frame

with $EA = 200m_c g$. Fig. 4(b) indicates that when the acceleration amplitude of the 1.44-s-long Ricker pulse is increased to $a_p = 0.53$ g (that is, a most strong excitation), the freestanding rocking frame is at the verge of overturning; however, its stability is appreciably enhanced even with the use of relative flexible restrainers (say $EA = 50m_c g$) that maintain a negative lateral stiffness.

Now the case of a 24-m-tall bridge pier with $2b = 4.0$ m ($R = 12.17$ m, $p = 0.778$ rad/s, and $\tan \alpha = 4/24 = 0.166$) is considered. Such tall piers are common in valley bridges (Makris et al. 2010). Again assume that this rocking frame with $p = 0.778$ rad/s, $\tan \alpha = 0.166$, and $\gamma = 4$ is excited by a Ricker pulse with $a_p = 0.35$ g and $T_p = 1.44$ s. This gives $\Pi_\omega = \omega_p/p = 2\pi/pT_p = 5.61$. For such a value of ω_p/p , the freestanding rocking frame with 24×4 -m piers survives the 1.44-s-long acceleration pulse even when its acceleration amplitude is as high as $a_p = 0.705$ g, as shown in Fig. 4(c). The main conclusion that emerges from Fig. 4 is that as the size of the columns (or the frequency of the excitation) increases, the effect of the vertical restrainers becomes immaterial given that most of the seismic resistance originates from the mobilization of the rotational inertia of the columns.

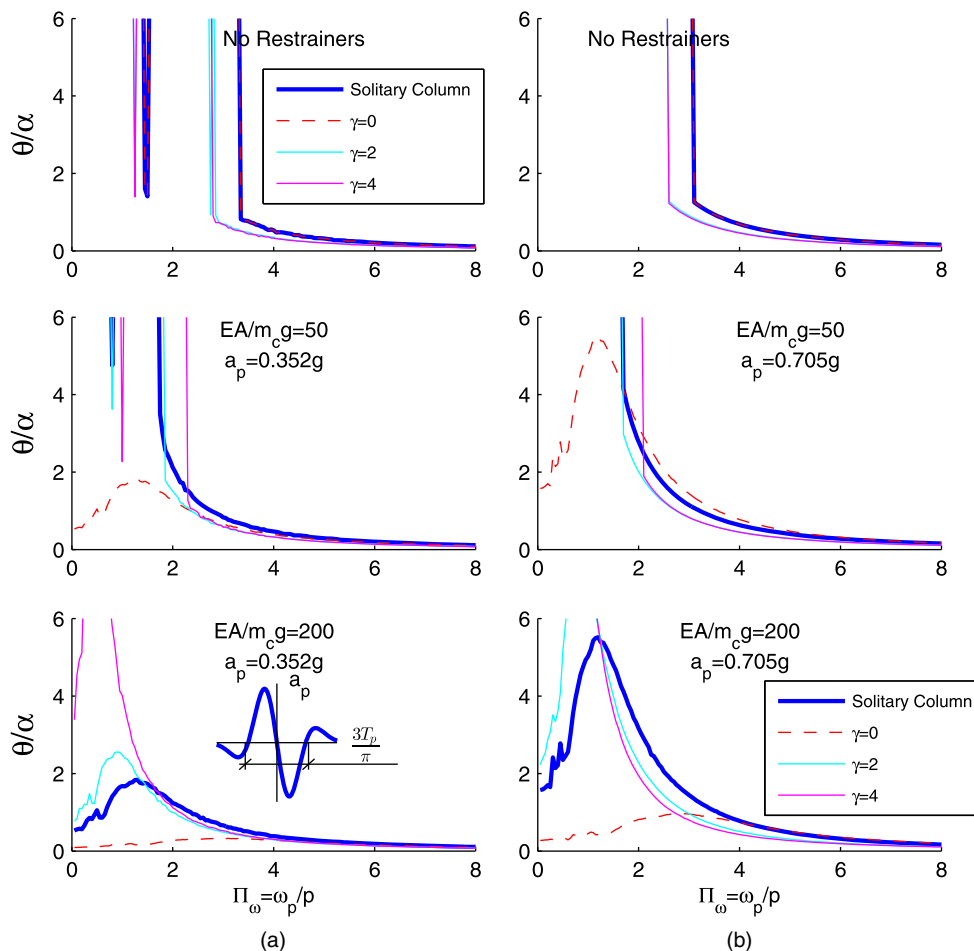


Fig. 5. Rocking spectra for different values of the dimensionless products $\Pi_g = a_p/g$, $\Pi_E = EA/m_c g$, and $\Pi_\gamma = \gamma$ when a vertically restrained rocking frame with columns having slenderness $\alpha = 10^\circ$ ($\Pi_\alpha = \tan \alpha = 0.176$) and $P_o = 0$ is subjected to an antisymmetric Ricker wavelet; in tall rocking frames (large values of ω_p/p) the effect of vertical restrainers is marginal: (a) $\Pi_g/\Pi_\alpha = a_p/g \tan \alpha = 2$; (b) $\Pi_g/\Pi_\alpha = a_p/g \tan \alpha = 4$

Equivalent Rigid-Linear System

Eq. (20) describes the full nonlinear dynamic response of the vertically restrained rocking frame. During rocking motion the restoring moment rides one of the moment-rotation curves shown in Figs. 2(c and d) without enclosing any area; energy is dissipated only during impact because the postimpact angular velocity is \sqrt{r} times the preimpact angular velocity. The theoretical maximum value of the coefficient of restitution, r , ensures that the rocking motion is given by Eq. (21). In this section an equation of motion is derived, equivalent to Eq. (20), which corresponds to a rigid-linear single-degree-of-freedom system. With this equivalent equation, the response of the vertically restrained rocking frame can be easily computed with open-source or commercially available software such as *OpenSees* (Mazzoni et al. 2006) simply by employing existing elastic-multilinear elements. This analysis investigates separately the cases for $\theta(t) < 0$ and $\theta(t) > 0$. Eq. (15)—that is, $\theta(t) < 0$ can be expressed as

$$\frac{1}{p^2} \frac{1+3\gamma}{1+2\gamma} \ddot{\theta} + \sin \alpha \left[-\cos \theta + \sin \theta \left(\frac{2}{1+2\gamma} \tan \alpha \frac{EA}{m_c g} + \frac{2}{1+2\gamma} \frac{1}{\sqrt{2}\sqrt{1-\cos \theta}} \frac{P_o}{m_c g} - \cot \alpha \right) \right] = -\frac{\ddot{u}_g}{g} \cos(\alpha + \theta) \quad (41)$$

where $p^2 = 3g/4R$.

For small values of θ $1 - \cos \theta \approx \theta^2/2$; in this case $\theta(t) < 0$. Accordingly, for $\theta(t) < 0$, $\sqrt{2}\sqrt{1 - \cos \theta} \approx |\theta|$ and Eq. (41) assumes the form

$$\frac{1}{p^2} \frac{1+3\gamma}{1+2\gamma} \ddot{\theta} + \sin \alpha \left[-\cos \theta + \frac{\sin \theta}{|\theta|} \frac{2}{1+2\gamma} \frac{P_o}{m_c g} + \sin \theta \left(\frac{2}{1+2\gamma} \tan \alpha \frac{EA}{m_c g} - \cot \alpha \right) \right] = -\frac{\ddot{u}_g}{g} \cos(\alpha + \theta) \quad (42)$$

Eq. (42) is further linearized up to first-order terms by taking $\sin \theta \approx \theta$ and $\cos \theta = \cos(\alpha + \theta) \approx 1$; recall that the frequency parameter of the rocking frame is $\hat{p} = p(1+2\gamma)/(1+3\gamma)$

$$\ddot{\theta}(t) - \hat{p}^2 \sin \alpha \left(1 + \frac{2}{1+2\gamma} \frac{P_o}{m_c g} \right) + \omega_r^2 \theta(t) = -\hat{p}^2 \frac{\ddot{u}_g(t)}{g} \quad (43)$$

In Eq. (43), ω_r^2 is given by Eq. (38). When $EA/m_c g$ is sufficiently large and satisfies Eq. (26), the linear branch of the stiffness of the system shown at the bottom in Fig. 2 is positive and ω_r is the system's natural frequency. When $EA/m_c g$ does not satisfy Eq. (26), ω_r^2 is negative and the system's free-vibration response is described by hyperbolic sines and cosines (Makris and Roussos 2000).

For positive rotations [$\theta(t) > 0$], following a similar derivation yields

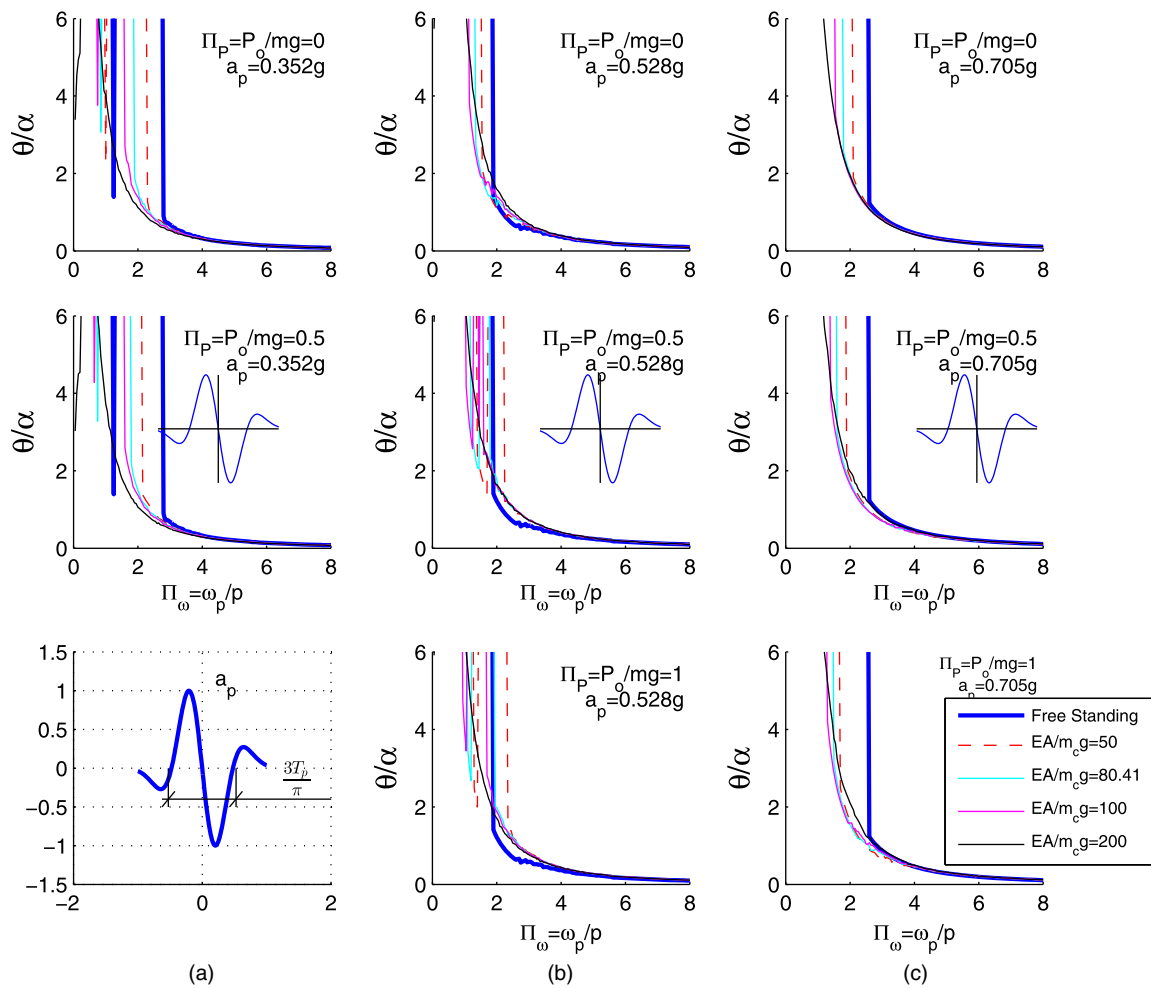


Fig. 6. Rocking spectra, $\Pi_\alpha = \tan \alpha = 0.176$ ($\alpha = 10^\circ$), $\Pi_\gamma = \gamma = 4$, for different values of the dimensionless products; $\Pi_g = a_p/g$, $\Pi_E = EA/m_c g$, and $\Pi_p = P_o/m_c g$ when the vertically restrained rocking frame with column slenderness $\alpha = 10^\circ$ ($\Pi_\alpha = \tan \alpha = 0.176$) and $\Pi_\gamma = \gamma = 4$ is subjected to an antisymmetric Ricker wavelet; for values of $\Pi_\omega = \omega_p/p > 3$, the response of the freestanding rocking frame is essentially identical to the response of the restrained frame, showing that for tall rocking frames the effect of vertical restrainers is marginal; (a) $\Pi_g/\Pi_\alpha = a_p/g \tan \alpha = 2$; (b) $\Pi_g/\Pi_\alpha = a_p/g \tan \alpha = 3$; (c) $\Pi_g/\Pi_\alpha = a_p/g \tan \alpha = 4$

$$\ddot{\theta} + \hat{p}^2 \sin \alpha \left(1 + \frac{2}{1 + 2\gamma} \frac{P_o}{m_c g} \right) + \omega_r^2 \theta = -p^2 \frac{\ddot{u}_g}{g} \quad (44)$$

Eqs. (43) and (44) can be combined in a single equation that describes a rigid-linear system with either positive ($\omega_r^2 > 0$) or negative ($\omega_r^2 < 0$) stiffness:

$$\ddot{\theta}(t) + \hat{p}^2 \sin \alpha \left(1 + \frac{2}{1 + 2\gamma} \frac{P_o}{m_c g} \right) \text{sgn} \theta(t) + \omega_r^2 \theta(t) = -\hat{p}^2 \frac{\ddot{u}_g}{g} \quad (45)$$

where $\text{sgn} \theta = \text{sign}$ of the rotation of the vertically restrained rocking frame. On uplifting, Eq. (45) becomes a linear equation and describes a special case of the wide class of multilinear-elastic systems (Kam et al. 2010). Eq. (45) shows in a direct way the increasing stability of a rocking frame as the size of its columns increases (smaller values of p) because, according to the dynamics of rocking, the apparent input excitation is suppressed with the square of the frequency parameter [$\hat{p}^2(\ddot{u}_g/g)$].

Eq. (45) describes the rigid-linear behavior of a single DOF system schematically shown at the bottom in Fig. 2. Given that the rigid linear curves do not enclose any area, the equation describes

the response of an undamped system. Rocking frames dissipate energy during impact, and research-oriented codes account for this energy loss by reducing the angular velocity of the column just after the impact according to some coefficient of restitution [e.g., Eq. (21)]. In routine structural engineering software, which offers elastic-multilinear elements, the capability of detecting the instant of impact to reduce the angular velocity is limited; therefore, there is a need for inserting some equivalent linear damping proportional to the angular velocity. An equivalent linear damping of the form $c\dot{\theta}$ needs to have the same units as $I\ddot{\theta}$. Accordingly, the units of the damping coefficient, c , are $[M][L]^2[T]^{-1}$. Formal dimensional analysis gives that (Vassiliou et al. 2014)

$$c = \lambda m_c g^{1/2} R^{3/2} \quad (46)$$

where $\lambda = \text{unknown scalar quantity}$ to be determined from the best fit of the nonlinear rocking response. From Eq. (46) and after recalling that $p^2 = m_c g R / I_o$, it is determined that, for rectangular columns ($p = \sqrt{3g/4R}$), the damping coefficient of the angular velocity, $\dot{\theta}(t)$, is $c/I_o = \sqrt{(3/4)\lambda} p$. About a decade ago, Makris and Konstantinidis (2003) proposed an empirical expression for the equivalent viscous damping ratio, $\beta = -0.34 \ln(r)$ that is needed to account for the decay of the free vibrations of freestanding rocking

columns. This empirical expression, $\beta = -0.34 \ln(r)$ was subsequently validated experimentally by Cheng (2007). Given the direct correspondence between the rocking frame and a taller solitary freestanding column (Makris and Vassiliou 2013), the scalar coefficient $\sqrt{(3/4)\lambda}$ can be replaced with $2\beta = -0.68 \ln(r)$, where r is the coefficient of restitution needed to sustain the rocking motion as offered by Eq. (21).

Based on the previous discussion, the undamped Eq. (45), which describes the response of a rigid-linear system, can be upgraded to a damped equation in an effort to approximate the damped response of the rocking frame

$$\ddot{\theta}(t) + 0.68 \ln(r) \hat{p} \dot{\theta}(t) + \hat{p}^2 \sin \alpha \left(1 + \frac{2}{1 + 2\gamma m_c g} \frac{P_o}{m_c g} \right) \text{sgn} \theta(t) + \omega_r^2 \theta(t) = -\hat{p}^2 \frac{\ddot{u}_g}{g} \quad (47)$$

Fig. 7 plots the rotation response histories of a smaller bridge rocking frame (9.6-m-tall columns) and a larger bridge rocking frame (24-m-tall columns) when subjected to the Takarazuka/000 ground motion recorded during the 1995 Kobe, Japan, Earthquake. The slenderness of the columns in both frames is $\Pi_\alpha = \tan \alpha = 0.166$ and $\gamma = m_b / Nm_c = 4$. The heavy lines show the response obtained with the full nonlinear Eq. (20); the thin lines show the response obtained with the viscously damped, equivalent rigid-linear elements described by Eq. (47). In all cases, the peak rotations calculated with the equivalent rigid-linear system are in very good agreement with the rigorous nonlinear solution given by Eq. (20) whereas the response history of the equivalent rigid-linear system appears to be underdamped. In any event, the rotation history predicted with the equivalent rigid-linear system is on the conservative side. Fig. 7 shows that both rocking frames exhibit comparable peak rotations regardless of whether they are freestanding or restrained with restrainers that are as stiff

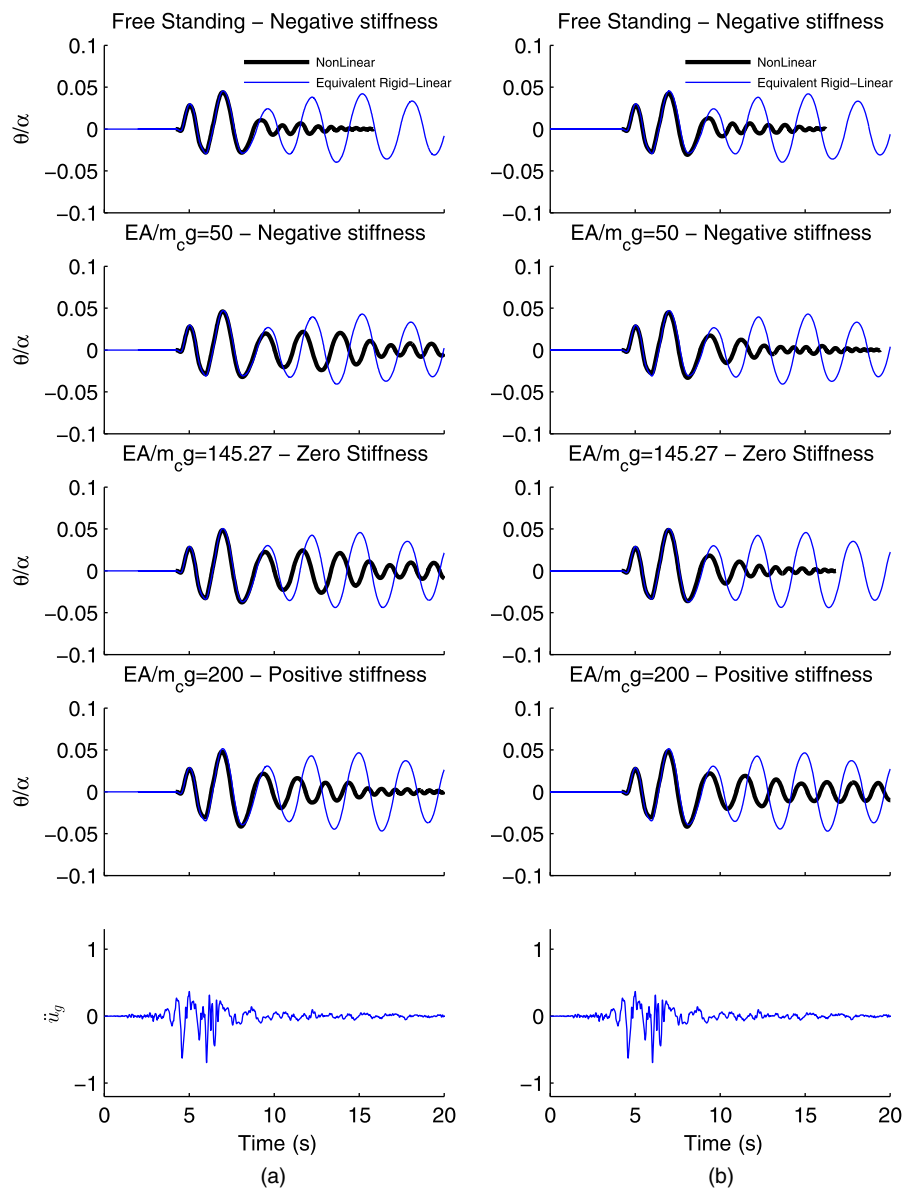


Fig. 7. Rotation response histories for Takarazuka/000 ground motion recorded during the 1995 Kobe, Japan, Earthquake: (a) medium-size rocking frame supported on 9.6-m-tall columns: $2h = 9.60$ m, $p = 1.23$ rad/s; (b) larger rocking frame supported on 24-m-tall columns: $2h = 24$ m, $p = 0.777$ rad/s; the peak rotation of both rocking frames is essentially independent of the axial stiffness of the restrainers

as $EA/m_c g = 200$. This is because most of the seismic resistance of tall rocking frames originates from the difficulty in mobilizing the large rotational inertia of the tall columns (proportional to R^2) whereas the effect of the vertical restrainers becomes marginal.

Conclusions

This paper investigates the rocking response and stability of an array of slender columns capped with a rigid beam which are vertically restrained with elastic prestressed tendons that pass through the centerlines of the columns. Whereas the lateral stiffness of a free-standing rocking frame is negative, the lateral stiffness of a vertically restrained rocking frame can be anywhere from negative to positive depending on the axial stiffness of the restraining tendons.

Following a variational formulation, the paper shows that the restraining tendons are effective in suppressing the response of rocking frames with small columns when subjected to long-period excitations. As the size of the columns, the frequency of the excitation, or the weight of the cap beam increases, the vertical restraining tendons become immaterial given that most of the seismic resistance of tall rocking frames originates primarily from the mobilization of the rotational inertia of their columns.

The paper also shows that for rocking frames up to a medium size, where the concept of vertical restrainers may be attractive, there is engineering merit in the vertical tendons being flexible enough that the overall lateral stiffness of the rocking frame remains negative. In this way, the pivot points are not overloaded with high compressive forces but the rocking structure enjoys ample seismic stability by avoiding resonance because of the negative stiffness.

Finally, the paper proposes and validates a rigid linear system whose dynamic response is equivalent to that of the vertically restrained rocking frame. With this equivalent system, the dynamic response of a vertically restrained rocking frame can be easily computed with popular open-source or commercially available software simply by employing the ready-to-use elastic-multilinear element. It is recommended that the final design of a rocking structure be validated with time-history analysis using the methodology presented here.

Acknowledgments

This work was funded by the research project Seismo-Rock Bridge with Grant No. 2295, which is implemented under the ARISTEIA action of OPERATIONAL PROGRAMME EDUCATION AND LIFELONG LEARNING and is cofunded by the European Social Fund (ESF) and Greek National Resources.

References

Alavi, B., and Krawinkler, H. (2001). "Effects of near-source ground motions on frame-structures." *Technical Rep. No. 138*, John A. Blume Earthquake Engineering Center, Stanford Univ., Stanford, CA.

Ambraseys, N., and Psycharis, I. N. (2011). "Earthquake stability of columns and statues." *J. Earthquake Eng.*, 15(5), 685–710.

Apostolou, M., Gazetas, G., and Garini, E. (2007). "Seismic response of slender rigid structures with foundation uplifting." *Soil Dyn. Earthquake Eng.*, 27(7), 642–654.

Baker, J. W. (2007). "Quantitative classification of near-fault ground motions using wavelet analysis." *Bull. Seismol. Soc. Am.*, 97(5), 1486–1501.

Beck, J. L., and Skinner, R. I. (1973). "The seismic response of a reinforced concrete bridge pier designed to step." *Earthquake Eng. Struct. Dyn.*, 2(4), 343–358.

Bertero, V. V., Mahin, S. A., and Herrera, R. A. (1978). "Aseismic design implications of near-fault San Fernando earthquake records." *Earthquake Eng. Struct. Dyn.*, 6(1), 31–42.

Chen, Y. H., Liao, W. H., Lee, C. L., and Wang, Y. P. (2006). "Seismic isolation of viaduct piers by means of a rocking mechanism." *Earthquake Eng. Struct. Dyn.*, 35(6), 713–736.

Cheng, C. T. (2007). "Energy dissipation in rocking bridge piers under free vibration tests." *Earthquake Eng. Struct. Dyn.*, 36(4), 503–518.

Cheng, C. T. (2008). "Shaking table tests of a self-centering designed bridge substructure." *Eng. Struct.*, 30(12), 3426–3433.

Cohagen, L., Pang, J. B. K., Stanton, J. F., and Eberhard, M. O. (2008). "A precast concrete bridge bent designed to recenter after an earthquake." *Research Rep.*, Federal Highway Administration, Washington, DC.

DeJong, M. J., and Dimitrakopoulos, E. G. (2014). "Dynamically equivalent rocking structures." *Earthquake Eng. Struct. Dyn.*, 43(10), 1543–1563.

Hall, J. F., Heaton, T. H., Halling, M. W., and Wald, D. J. (1995). "Near-source ground motion and its effects on flexible buildings." *Earthquake Spectra*, 11(4), 569–605.

Kam, W. Y., Pampanin, S., Palermo, A., and Carr, A. J. (2010). "Self-centering structural systems with combination of hysteretic and viscous energy dissipations." *Earthquake Eng. Struct. Dyn.*, 39(10), 1083–1108.

Karavasilis, T. L., Makris, N., Bazeos, N., and Beskos, D. E. (2010). "Dimensional response analysis of multistory regular steel MRF subjected to pulselike earthquake ground motions." *J. Struct. Eng.*, 10.1061/(ASCE)ST.1943-541X.0000193, 921–932.

Konstantinidis, D., and Makris, N. (2005). "Seismic response analysis of multidrum classical columns." *Earthquake Eng. Struct. Dyn.*, 34(10), 1243–1270.

Mahin, S., Sakai, J., and Jeong, H. (2006). "Use of partially prestressed reinforced concrete columns to reduce post-earthquake residual displacements of bridges." *5th National Seismic Conf. on Bridges & Highways*, San Francisco.

Makris, N. (1997). "Rigidity–plasticity–viscosity: Can electrorheological dampers protect base-isolated structures from near-source ground motions?" *Earthquake Eng. Struct. Dyn.*, 26(5), 571–591.

Makris, N. (2014). "The role of the rotational inertia on the seismic resistance of free-standing rocking columns and articulated frames." *Bull. Seismol. Soc. Am.*, 104(5), 2226–2239.

Makris, N., and Black, C. J. (2002). "Uplifting and overturning of equipment anchored to a base foundation." *Earthquake Spectra*, 18(4), 631–661.

Makris, N., and Black, C. J. (2004a). "Dimensional analysis of bilinear oscillators under pulse-type excitations." *J. Eng. Mech.*, 10.1061/(ASCE)0733-9399(2004)130:9(1019), 1019–1031.

Makris, N., and Black, C. J. (2004b). "Dimensional analysis of rigid-plastic and elastoplastic structures under pulse-type excitations." *J. Eng. Mech.*, 10.1061/(ASCE)0733-9399(2004)130:9(1006), 1006–1018.

Makris, N., and Chang, S.-P. (2000). "Effect of viscous, viscoplastic and friction damping on the response of seismic isolated structures." *Earthquake Eng. Struct. Dyn.*, 29(1), 85–107.

Makris, N., Kampas, G., and Angelopoulou, D. (2010). "The eigenvalues of isolated bridges with transverse restraints at the end abutments." *Earthquake Eng. Struct. Dyn.*, 39(8), 869–886.

Makris, N., and Konstantinidis, D. (2003). "The rocking spectrum and the limitations of practical design methodologies." *Earthquake Eng. Struct. Dyn.*, 32, 265–289.

Makris, N., and Psychogios, T. (2006). "Dimensional response analysis of yielding structures with first-mode dominated response." *Earthquake Eng. Struct. Dyn.*, 35(10), 1203–1224.

Makris, N., and Roussos, Y. S. (2000). "Rocking response of rigid blocks under near-source ground motions." *Geotechnique*, 50(3), 243–262.

Makris, N., and Vassiliou, M. F. (2013). "Planar rocking response and stability analysis of an array of free-standing columns capped with a freely supported rigid beam." *Earthquake Eng. Struct. Dyn.*, 42(3), 431–449.

Makris, N., and Vassiliou, M. F. (2014). "Are some top-heavy structures more stable?" *J. Struct. Eng.*, 10.1061/(ASCE)ST.1943-541X.0000933, 06014001.

- Makris, N., and Zhang, J. (2001). "Rocking response of anchored blocks under pulse-type motions." *J. Eng. Mech.*, 10.1061/(ASCE)0733-9399(2001)127:5(484), 484–493.
- Makris, N., and Zhang, J. (2004). "Seismic response analysis of a highway overcrossing equipped with elastomeric bearings and fluid dampers." *J. Struct. Eng.*, 10.1061/(ASCE)0733-9445(2004)130:6(830), 830–845.
- Mander, J. B., and Cheng, C. T. (1997). "Seismic resistance of bridge piers based on damage avoidance design." *Technical Rep. NCEER, 97*, National Center for Earthquake Engineering Research, State Univ. of New York at Buffalo, Buffalo, NY.
- Mavroeidis, G. P., and Papageorgiou, A. S. (2003). "A mathematical representation of near-fault ground motions." *Bull. Seism. Soc. Am.*, 93(3), 1099–1131.
- Mazzoni, S., McKenna, F., Scott, M. H., and Fenves, G. L. (2006). "OpenSees command language manual." Pacific Earthquake Engineering Research Center, Univ. of California at Berkeley, Berkeley, CA.
- Palermo, A., Pampanin, S., and Calvi, G. M. (2005). "Concept and development of hybrid solutions for seismic resistant bridge systems." *J. Earthquake Eng.*, 9(6), 899–921.
- Papaloizou, L., and Komodromos, P. (2009). "Planar investigation of the seismic response of ancient columns and colonnades with epistyles using a custom-made software." *Soil Dyn. Earthquake Eng.*, 29(11), 1437–1454.
- Pasala, D. T. R., Sarlis, A. A., Nagarajaiah, S., Reinhorn, A. M., Constantinou, M. C., and Taylor, D. (2012). "Adaptive negative stiffness: New structural modification approach for seismic protection." *J. Struct. Eng.*, 10.1061/(ASCE)ST.1943-541X.0000615, 1112–1123.
- Pecker, A. (2005). "Design and construction of the foundations of the Rion Antirion Bridge." *Proc., 1st Greece—Japan Workshop on Seismic Design, Observation, Retrofit of Foundations*, Athens, Greece, 119–130.
- Ricker, N. (1943). "Further developments in the wavelet theory of seismogram structure." *Bull. Seismol. Soc. Am.*, 1943(33), 197–228.
- Ricker, N. (1944). "Wavelet functions and their polynomials." *Geophysics*, 9(3), 314–323.
- Sakai, J., Jeong, H., and Mahin, S. A. (2006). "Reinforced concrete bridge columns that re-center following earthquakes." *8th U.S. National Conf. on Earthquake Engineering 100th Anniversary Earthquake Conf.*, San Francisco.
- Sarlis, A. A., Pasala, D. T. R., Constantinou, M. C., Reinhorn, A. M., Nagarajaiah, S., and Taylor, D. P. (2012). "Negative stiffness device for seismic protection of structures." *J. Struct. Eng.*, 10.1061/(ASCE)ST.1943-541X.0000616, 1124–1133.
- Sharpe, R. D., and Skinner, R. I. (1983). "The seismic design of an industrial chimney with rocking base." *Bull. New Zealand National Soc. Earthquake Eng.*, 19(2), 98–106.
- Vassiliou, M. F. (2010). "Analytical investigation of the dynamic response of a pair of columns capped with a rigid beam and of the effect of seismic isolation on rocking structures." Ph.D. dissertation, Dept. of Civil Engineering, Univ. of Patras, Greece (in Greek).
- Vassiliou, M. F., Mackie, K. R., and Stojadinović, B. (2014). "Dynamic response analysis of solitary flexible rocking bodies: Modeling and behavior under pulse-like ground excitation." *Earthquake Eng. Struct. Dyn.*, 43(10), 1463–1481.
- Vassiliou, M. F., and Makris, N. (2011). "Estimating time scales and length scales in pulselike earthquake acceleration records with wavelet analysis." *Bull. Seismol. Soc. Am.*, 101(2), 596–618.
- Vassiliou, M. F., and Makris, N. (2012). "Analysis of the rocking response of rigid blocks standing free on a seismically isolated base." *Earthquake Eng. Struct. Dyn.*, 41(2), 177–196.
- Veletsos, A. S., and Newmark, N. M. (1960). "Effect of inelastic behavior on the response of simple systems to earthquake motions." *Proc., 2nd World Conf. on Earthquake Engineering*, Tokyo, 895–912.
- Veletsos, A. S., Newmark, N. M., and Chelepati, C. V. (1965). "Deformation spectra for elastic and elastoplastic systems subjected to ground shock and earthquake motions." *Proc., 3rd World Conf. on Earthquake Engineering*, Vol. II, Wellington, New Zealand, 663–682.
- Wacker, J. M., Hieber, D. G., Stanton, J. F., and Eberhard, M. O. (2005). "Design of precast concrete piers for rapid bridge construction in seismic regions." *Research Rep.*, Federal Highway Administration, Washington, DC.
- Zhang, J., Makris, N., and Delis, T. (2004). "Structural characterization of modern highway overcrossings: Case study." *J. Struct. Eng.*, 10.1061/(ASCE)0733-9445(2004)130:6(846), 846–860.